JOURNAL OF CATALYSIS 84, 178–188 (1983)

Impregnation of Alumina with Copper Chloride-Modeling of Impregnation Kinetics and Internal Copper Profiles

ALFONS BAIKER[1] AND WILLIAM L. HOLSTEIN[2]

Swiss Federal Institute of Technology (ETH), Department of Industrial and Engineering Chemistry, CH-8092, Zurich, Switzerland

Received March 23, 1983; revised June 13, 1983

The impregnation of previously wetted alumina pellets with aqueous solution of copper(II) chloride is studied experimentally and theoretically. Internal copper concentration profiles resulting from impregnation with different copper chloride solution concentrations and various impregnation times are determined by electron probe microanalysis and indicate a shell-progressive immobilization. Temperature-programmed reduction measurements conducted on impregnated alumina catalysts indicate two types of immobilized copper species with different reducibilities. An impregnation model is applied to describe the experimentally determined internal copper concentration profiles and the copper uptakes in terms of the measurable properties of the system. The model is based on slow diffusion and rapid irreversible immobilization of the copper ions on the support. It extends the well-known shell-progressive immobilization model to account for precipitation, which occurs during the drying process, of metal ions from solution trapped in the catalyst pores. Thus the model extends the scope of the shell-progressive model, which is applicable only for local metal loadings corresponding to the site density of immobilization sites, to the preparation of catalysts with higher local metal loadings. A tortuosity factor of 1.8 for the alumina support is calculated from the effective diffusivity of the copper chloride as estimated from the measured data and its molecular diffusivity as reported in the literature. The experimentally determined internal concentration profiles and copper uptakes agree with the theory to within experimental error.

INTRODUCTION

An important factor determining the activity and selectivity of a supported catalyst is the distribution of the active component throughout the support. This distribution is primarily determined at the steps of impregnation and drying. A comprehensive review of the chemical and physical processes affecting these steps has recently appeared (*1*).

Mathematical descriptions of the impregnation step have been given by several authors (*2–13*). However, only in a few investigations (*9, 10, 12*) have experimentally measured radial profiles of the active component been compared with those predicted with a mathematical model. Weisz *et al.* (*2–4*) developed a general diffusion–sorption model and applied it to the impregnation of porous substrates with dyes. This model was derived assuming constant concentration in the external impregnation solution. Harriott (*5*) generalized Weisz's model by considering the effect of external solution depletion during impregnation. Vincent and Merrill (*6*) presented a model to describe the filling of pores with a solute as it takes place with impregnation of a dry support. Melo *et al.* (*9, 10*) have reported models to describe the impregnation of both wetted and dry supports. They applied their models to measured internal concentration profiles obtained by impregnation of alumina with nickel nitrate and barium nitrate solutions.

In this work, a mathematical model is presented which describes the impregnation of a porous support with an active component, resulting from slow diffusion and rapid irreversible immobilization of the

[1] To whom all correspondence should be addressed.
[2] Present address: Du Pont, Experimental Station, Wilmington, Delaware 19898.

0021-9517/83 $3.00

active component. The previously described impregnation of γ-alumina with copper chloride (*14*) is employed as an example for modeling such an impregnation process.

The goal is to describe the experimentally determined internal concentration profiles and the total metal uptakes in terms of the measurable properties of the system. These properties are the geometric dimensions, the porosity, and the site density for irreversible immobilization of the support, as well as the impregnation time and the bath concentration of the impregnation solution. The effective diffusion coefficient of the metal ions into the support is estimated from the experimental data.

THEORY

The preparation of supported catalyst can be viewed as taking place in three steps: impregnation, drying, and thermotreatment (*1*). The impregnation of a previously wetted support involves diffusion of the metal ions into the support and their immobilization by the support. The impregnation of an unwetted support also involves convection of the impregnation solution into the support.

The catalyst support has a fixed number of immobilization sites. To prepare catalysts with higher metal loadings, an additional precipitation step must occur. One such method is the employment of a solution with a high concentration of metal ions. Metal ions present in the solute in the pores will then be precipitated upon drying. The drying process may also result in a redistribution of previously immobilized metal ions. When drying is slow, further diffusion and immobilization of metal ions present in the solute in the pores may also occur.

The thermal processing steps, such as calcination and reduction, generally have little effect on the macroscopic distribution of metal through the pellet. The effect is only on the local distribution and the resulting size of the individual particles produced. This step can be ignored in modeling the distribution of catalyst throughout the pellet.

The model developed below will include the impregnation and drying steps. Rapid, irreversible immobilization and rapid precipitation during drying are assumed.

Immobilization Process for a Previously Wetted Support

The simultaneous diffusion of catalyst ions into a previously wetted support and their immobilization on the support can be described by Eq. (1) which represents the conservation of material in each volume element.

$$\frac{\partial C}{\partial t} = D_e \nabla^2 C - r \tag{1}$$

where C (mol liter^{-1}) is the concentration of metal ions in the fluid; t (s) is time; D_e (cm^2 s^{-1}) is the effective diffusion coefficient for metal ions in the solute through the pellet; r (mol liter^{-1} s^{-1}) is the rate of catalyst immobilization.

For a constant bath concentration, C_0, the boundary conditions are $C = C_0$ at $R = R_0$, $t = 0$; $C = 0$ at $0 < R < R_0$, $t = 0$; $(\partial C/\partial R) = 0$ at $R = 0$, $t \geq 0$; where R_0 is the pellet radius. If the time scale for immobilization is much less than the time scale for diffusion, as is frequently the case for catalyst preparation, the concentration of metal ions in the liquid phase, C, may be assumed to be equilibrated with the concentration of immobilized metal ions on the support, S. Two types of adsorption isotherms have been previously considered. The first considers a Langmuir adsorption isotherm of the form

$$S = S_0 \left(\frac{KC}{1 + KC}\right) \tag{2}$$

where S_0 (mol kg^{-1}) is the concentration of possible immobilization sites on the support and K (liter mol^{-1}) is the equilibrium constant for the immobilization process. When S is linearly related to C ($KC \ll 1$), Eq. (1)

can be solved analytically (*15*). A numerical solution is possible otherwise (*2, 3*). The second model assumes that adsorption is rapid and irreversible ($S = S_0$ for $C > 0$; $S = 0$ for $C = 0$). This mathematical problem can be solved analytically (*16*).

The assumption of a Langmuir isotherm results in a concentration profile of the immobilized metal with a somewhat diffuse leading edge. By contrast, rapid, irreversible immobilization results in a sharp leading edge. The presence of a sharp leading edge in the data considered later in this paper led to the consideration of a catalyst impregnation model based on fast, irreversible immobilization. This type of model, also called a "shell progressive" or "shrinking core" model, has previously found application for the reduction of iron oxide (*17*) and the combustion of carbonaceous deposits in porous pellets (*18*). In one study it was applied to the preparation of supported metal catalysts, but only with regard to relating the impregnation front radius to the impregnation time (*8*).

Solution of the mathematical problem will be derived here for an infinite cylinder. The results for a flat slab and a sphere are then presented. For rapid, irreversible immobilization, it can be assumed that a steady-state concentration profile of metal ions exists in the liquid within the pellet (*1*). For a cylindrical pellet, the flux of ions into the cylinder of radius R_b, the impregnation front radius, is equal to the rate of adsorption

$$\frac{dN}{dt} = 2\pi L R_b D_e \left(\frac{dC}{dR}\right)_{R=R_b} \tag{3}$$

where dN/dt (mol s^{-1}) is the rate of immobilization and L is the length of the pellet. Between the impregnation radius, R_b, and the outer radius, R_0, the flux is constant

$$2\pi L D_e R \left(\frac{dC}{dR}\right) = \text{constant} \qquad R_b < R < R_0 \tag{4}$$

and the boundary conditions are

$C = 0$	$R = R_b$	$t > 0$
$C = C_0$	$R = R_0$	$t \geq 0$
$C = 0$	$0 < R < R_0$	$t = 0$

The problem can be put into dimensionless form by the following dimensionless relationships

$$C^* = C/C_0;\ t^* = \frac{tD_e}{R_0^2};$$

$$R^* = R/R_0;\ N^* = \frac{N}{C_0 V} \tag{5}$$

$$\frac{dN^*}{dt^*} = \frac{dN}{dt}\frac{R_0^2}{VC_0D_e} \tag{6}$$

where the pellet volume, V, for a cylinder is $V = \pi R_0^2 L$ Equations (3) and (4) become now

$$\frac{dN^*}{dt^*} = 2R_b^*\left(\frac{dC^*}{dR^*}\right)_{R^*=R_b^*} \tag{7}$$

$$R^*\frac{dC^*}{dR^*} = \text{constant} \qquad R_b^* < R^* < 1 \tag{8}$$

with the boundary conditions

$C^* = 0$	$R^* = R_b^*$	$t^* > 0$
$C^* = 1$	$R^* = 1$	$t^* \geq 0$
$C^* = 0$	$0 < R^* < 1$	$t^* = 0$

Solution of Eq. (8) with the first two boundary conditions yields the concentration profile of metal ions in the pore liquid when the impregnation radius has reached R_b^*.

$$C^* = 1 - \frac{\ln R^*}{\ln R_b^*} \qquad R_b^* < R^* < 1 \tag{9a}$$

$$C^* = 0 \qquad 0 < R^* < R_b^* \tag{9b}$$

Differentiation of Eq. (9a) and substitution into Eq. (7) yields

$$\frac{dN^*}{dt^*} = \frac{2}{\ln(1/R_b^*)} \tag{10}$$

The rate of immobilization is also equal to the rate of decrease of unoccupied immobi-

lization sites on the catalyst surface

$$\varepsilon \frac{dN}{dt} = 2\pi R_b L S_0 \rho (1 - \varepsilon) \left(\frac{-dR_b}{dt}\right) \quad (11a)$$

where ε is the void fraction of the pellet, and ρ is the solid density of the pellet material. In dimensionless form, this becomes

$$\frac{dN^*}{dt^*} = -2R_b^* \beta \left(\frac{dR_b^*}{dt^*}\right) \quad (11b)$$

where β is a dimensionless constant relating the concentration of immobilization sites to the concentration of metal ions; both normalized to account for the respective parts of the pellet which are solid and void.

$$\beta = \frac{S_0 \rho (1 - \varepsilon)}{C_0 \varepsilon} \quad (12)$$

Relating Eqs. (10) and (11b) and integrating with the boundary condition ($C^* = 0$; $0 < R^* < 1$; $t^* = 0$) yields a relationship between the impregnation radius, R_b^*, and time, t^*

$$t^* = \frac{\beta}{4} (R_b^{*2} \ln R_b^{*2} + 1 - R_b^{*2}) \quad (13)$$

When a previously wetted particle is dipped into a bath for a time t^*, Eq. (13) can be used to calculate the impregnation radius R_b^*. The local concentration of immobilized metal ions in the catalyst pellet, $S_i^* = S_i/S_0$, is then

$$S_i^* = 1 \qquad R_b^* \leq R^* < 1 \quad (14a)$$

$$S_i^* = 0 \qquad 0 < R^* < R_b^* \quad (14b)$$

The local concentration of metal ions in the pore liquid is given by Eqs. (9a) and (9b).

The Drying Step

When removed from the bath, the pellet contains two forms of metal ions, that which has been immobilized during the impregnation and that which is still present in the solution in the pores. Here we will deal with the contribution of the latter to the final concentration profile of the catalyst. The case will be analyzed for rapid precipitation during drying. Under such conditions, diffusion of metal ions within the pellet due to the existing concentration gradient will not be significant. It will also be assumed that convection of metal ions over long distances is not important.

Under the limitations imposed above, the metal ions in solution will be deposited on the pellet at the same radius at which they were when the pellet was removed from the bath. The local concentration of catalyst on the pellet resulting from this precipitation, S_p (mol kg^{-1}) is given by

$$S_p = \frac{C}{\rho} \frac{\varepsilon}{1 - \varepsilon} \quad (15a)$$

or in dimensionless form

$$S_p^* = \frac{S_p}{S_0} = \frac{C^*}{\beta} \quad (15b)$$

where C^* is given by Eqs. (9a) and (9b).

The total local concentration of catalyst in the pellet, S_t, is defined in terms of its dimensionless counterpart S_t^*

$$S_t^* = \frac{S_t}{S_0} \quad (16)$$

by taking into account catalyst deposited by both immobilization and precipitation during drying.

$$S_t^* = S_i^* + S_p^* \quad (17)$$

Referring to Eqs. (14a), (14b), and (15b), this yields

$$S_t^* = 1 + \frac{1}{\beta} \left(1 - \frac{\ln R^*}{\ln R_b^*}\right) \qquad R_b^* < R^* < 1 \quad (18a)$$

$$S_t^* = 0 \qquad 0 < R^* < R_b^* \quad (18b)$$

The uptake of metal by the whole pellet due to immobilization, N_i (mol kg^{-1}), and precipitation, N_p (mol kg^{-1}), and the total uptake, N_t (mol kg^{-1}), can be derived in terms of their dimensionless counterparts:

$$N_i^* = \frac{N_i}{S_0}; \; N_p^* = \frac{N_p}{S_0}; \; N_t^* = \frac{N_t}{S_0} \quad (19)$$

by integrating the local concentrations through the pellet.

$$N_i^* = \int_0^1 R^* S_i^* dR^* \Big/ \int_0^1 R^* dR^* = 1 - R_b^{*2} \quad (20)$$

$$N_p^* = \int_0^1 R^* S_p^* dR^* \Big/ \int_0^1 R^* dR^* = \frac{1}{\beta}\left(1 + \frac{1 - R_b^{*2}}{2 \ln R_b^*}\right) \quad (21)$$

$$N_t^* = N_i^* + N_p^* \quad (22)$$

The above calculations can also be carried out analogously for spherical catalyst particles and flat slabs. The equations relating the impregnation front radius to the impregnation time, the local metal catalyst concentration to the radius and impregnation radius, and the total uptake to the impregnation radius for the three different geometries are summarized below. R_0 represents the radius for cylindrical and spherical pellets and is equal to one-half of the width for a slab. The radius or width is assumed to be much less than the length, so that end effects are negligible.

Cylindrical Pellet

$$t^* = \frac{\beta}{4}(R_b^{*2} \ln R_b^{*2} + 1 - R_b^{*2}) \quad (23)$$

$$S_t^* = 1 + \frac{1}{\beta}\left(1 - \frac{\ln R^*}{\ln R_b^*}\right) \qquad R_b^* < R^* < 1 \quad (24a)$$

$$S_t^* = 0 \qquad 0 < R^* < R_b^* \quad (24b)$$

$$N_t^* = (1 - R_b^{*2}) + \frac{1}{\beta}\left(1 + \frac{1 - R_b^{*2}}{2 \ln R_b^*}\right) \quad (25)$$

Spherical Pellet

$$t^* = \beta\left(\frac{1}{6} + \frac{R_b^{*3}}{3} - \frac{R_b^{*2}}{2}\right) \quad (26)$$

$$S_t^* = 1 + \frac{1}{\beta}\left(\frac{1 - R_b^*/R^*}{1 - R_b^*}\right) \qquad R_b^* < R^* < 1 \quad (27a)$$

$$S_t^* = 0 \qquad 0 < R^* < R_b^* \quad (27b)$$

$$N_t^* = 1 - R_b^{*3} + \frac{1}{\beta}\left(\frac{3}{1 - R_b^*}\right)\left(\frac{1}{3} + \frac{R_b^{*3}}{6} - \frac{R_b^{*2}}{2}\right) \quad (28)$$

Flat Slab

$$t^* = \frac{\beta}{2}(1 - R_b^*)^2 \quad (29)$$

$$S_t^* = 1 + \frac{1}{\beta}\left(\frac{R^* - R_b^*}{1 - R_b^*}\right) \qquad R_b^* < R^* < 1 \quad (30a)$$

$$S_t^* = 0 \qquad 0 < R^* < R_b^* \quad (30b)$$

$$N_t^* = (1 - R_b^*) + \frac{1}{2\beta}(1 - R_b^*) \quad (31)$$

EXPERIMENTAL

Materials. Cylindrical γ-alumina pellets supplied by Girdler-Südchemie (type T-126) were employed as support material. The physical properties of the cylindrical alumina pellets of 4.3 × 4.3 mm size were: surface area (BET), 197 $m^2\ g^{-1}$; solid density, 3.43 g cm^{-3}; apparent density, 1.37 g cm^{-3}; void fraction, 0.60.

Figure 1 depicts the integral pore size distribution of the alumina pellets determined by nitrogen capillary condensation.

The impregnation solution was copper chloride ($CuCl_2 \cdot 2H_2O$) from Fluka AG (AR Grade) in aqueous solution.

Procedure. Before impregnation, the alumina pellets were wetted by soaking in distilled water at room temperature for 12 h. The impregnations were then carried out using a constant bath concentration at 25°C in a stirred bath containing 1 liter of $CuCl_2$ solution and 5 g alumina. After a defined impregnation time, the solution was drained off, and the pellets were quickly rinsed with distilled water and dried in an oven at 110°C for 24 h.

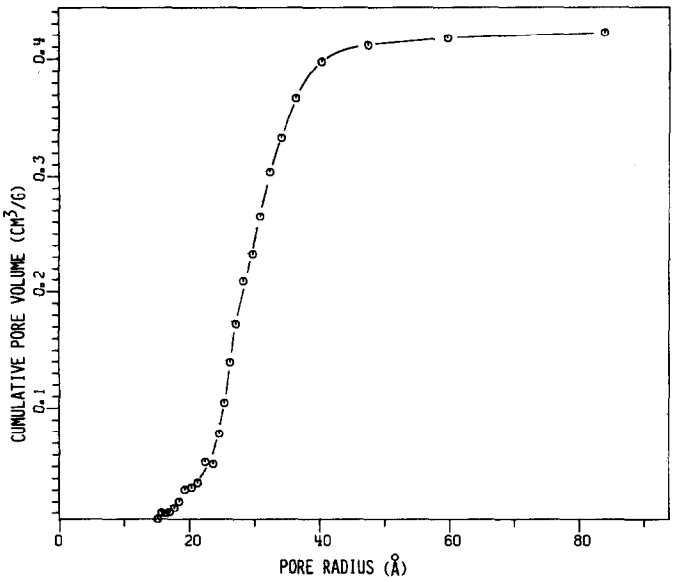

FIG. 1. Integral pore size distribution of alumina determined by nitrogen capillary condensation.

Determination of total uptake and internal copper profiles. The total uptake of $CuCl_2$ in the alumina support was determined spectrophotometrically after extraction of a number of pellets with 60% nitric acid. About 98% of the $CuCl_2$ was extracted after six extraction steps with aliquots of 60 wt% nitric acid at 60°C. For the spectrophotometric measurements, the total extract was diluted with distilled water to give a nitric acid content of 8%.

The internal copper distribution along the radius of the alumina pellets was measured by means of an electron probe microanalyzer (Novelco AMR-3) using a 12° take off angle of X-rays and a 15-kV acceleration voltage of electron beam. To calibrate the sensitivity of the analyzer for copper, two standard samples with known copper contents were prepared. Total copper contents of each sample were also measured by standard chemical analysis.

The impregnated pellets were mounted in plastic and cut to reveal their cross section. The polished sections were flat on a scale of micrometers, except for pits of varying size and number. Since these pits caused some points of the concentration profiles to scatter widely, smoothed profiles are shown in this paper.

Temperature-programmed reduction. The apparatus and experimental procedure employed for the TPR measurements were the same as described elsewhere (*19*). Before measurements the samples were heated for 3 h at 350°C in flowing nitrogen (1.25 cm^3/s NTP). The sample weight amounted to 0.65 g. A gas mixture of 6% hydrogen in nitrogen at a flow rate of 1.25 cm^3/s (NTP) was used and the heating rate was 0.17 K/s.

RESULTS

A series of photographs of the cut pellets as a function of impregnation time is shown in Fig. 2. The shell progressive nature of the process is apparent. The pictures also give some idea of the scatter in the measurement of the impregnation radius. The fact that the catalyst concentration is changing continuously between the impregnation radius and the outer radius is not apparent from the optical photographs.

When the impregnation front reaches the

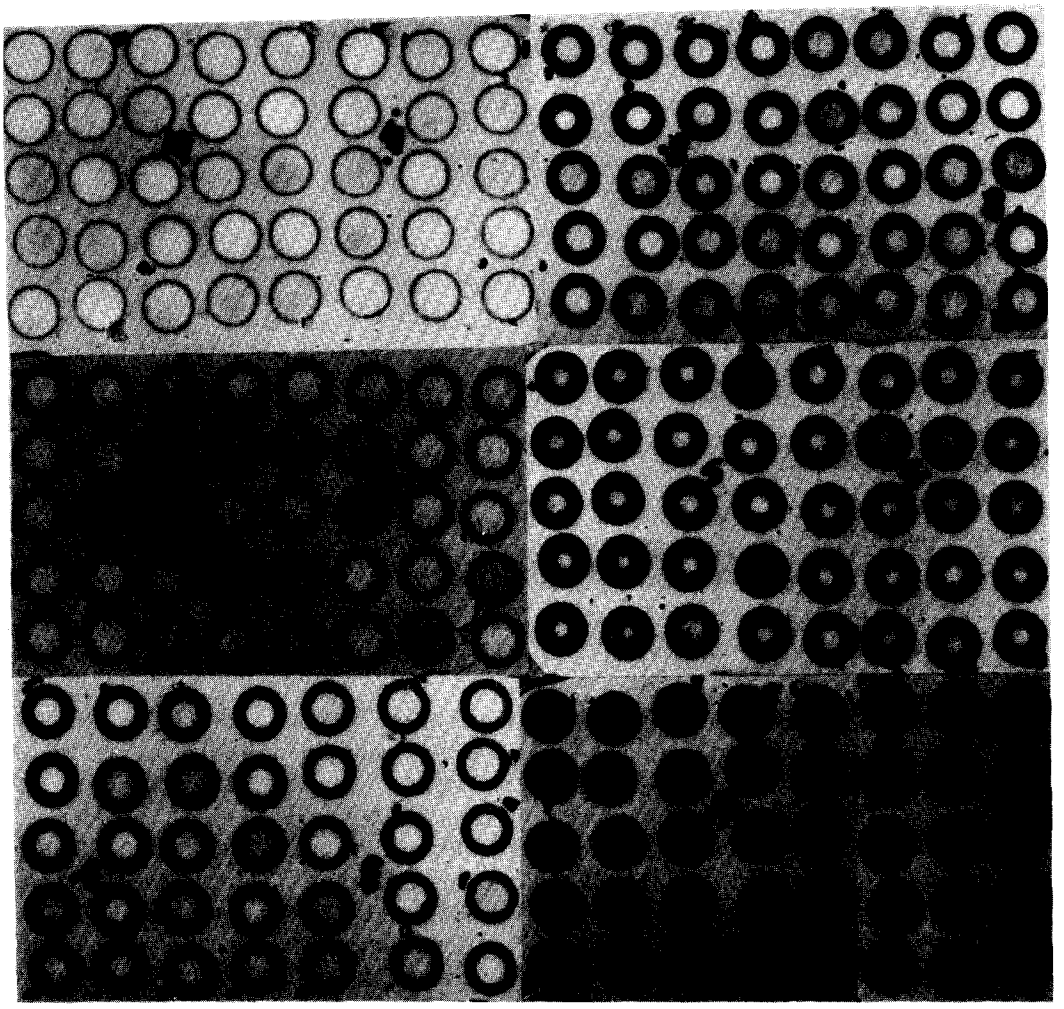

FIG. 2. Photographs of cut pellets impregnated with different impregnation times. Impregnation time increases from the top to the bottom. Pellets on the left side correspond to 10, 20, and 25 min, and those on the right to 35, 50, and 100 min impregnation. Bath concentration $C_0 = 0.5$ mol liter^{-1}.

center of the pellet, all of the immobilization sites are occupied, and the concentration of copper ions in solution in the pores of the pellet is considered to be uniform and equal to the concentration outside the pellet. Upon drying, the total uptake of the pellet is obtained from Eq. (25) for $R_b^* = 0$

$$N_t^* = 1 + \frac{1}{\beta}$$

or

$$N_t = S_0 + \frac{C_0 \cdot \varepsilon}{\rho(1 - \varepsilon)}$$

The site density for irreversible immobilization was determined in an earlier investigation (*14*) where uptake curves were measured as a function of the impregnation solution concentration. Extrapolating a plot of N_t vs C_0 to zero yielded a value for S_0 of 0.31 mol kg^{-1} (Fig. 6 in Ref. (*14*)).

The effective diffusion coefficient, D_e, can be calculated from the plot of (R_b^{*2} ln $R_b^{*2} + 1 - R_b^{*2}$) vs t shown in Fig. 3. Equations (13) and (5) indicate that the slope of the line should be $4D_e/\beta R_0^2$. For a bath concentration of 0.5 mol liter^{-1}, β is

$$\beta = \frac{(0.31 \times 10^{-3} \text{ mol g}^{-1})(3.43 \text{ g cm}^{-3})(1 - 0.60)}{(0.5 \times 10^{-3} \text{ mol cm}^{-3})(0.60)} = 1.42$$

With this information, D_e is calculated to be 3.1×10^{-6} cm^2 s^{-1}. From this calculated effective diffusivity, D_e, and the diffusivity, D, of copper(II) chloride reported in the literature (*20*), the tortuosity factor, τ, for the alumina pellets can be estimated using the relation $\tau = D\,\varepsilon/D_e$. The value so obtained of 1.8 agrees well with $\tau = \sqrt{3}$ as suggested in the literature (*21*).

The data fitting carried out throughout the rest of this work was done using the equations derived for cylindrical pellets, employing the above measured values of S_0 and D_e and the properties of the pellets as reported in the experimental section.

The calculated and experimental penetration radii are tabulated as a function of time in Table 1. The model fits the data within the experimental error, except for short times of less than 10 min. It appears that the diffusivity in the outermost shell of the pellet is slightly larger, probably due to an anisotropy effect caused by the pellet preparation.

The experimental and calculated concentration profiles are plotted as a function of dimensionless radius for different impregnation times and bath concentrations in Figs. 4 and 5. The agreement becomes less exact as the impregnation front approaches the center of the pellet, with the model predicting a slower approach than that measured experimentally. This results from two factors. First, the experimental method of measuring the concentration profiles tends to error on the side of underestimating the radius at low radii when measurement are made on a line not exactly intersecting the center of the pellet. Second, the assumption in the model that the cylindrical pellets are infinite in length becomes incorrect at small radii. The experimentally derived and calculated values of the total catalyst uptake as a function of time are presented in Table 2. The agreement is within the experimental error of measurement over the whole range of measurement. The model and theory agree even at low and high impregnation times. Since the uptake is not influenced by drying, the error resulting in the penetration radius at short impregnation times does not occur.

Figure 6 depicts the TPR profiles obtained for two alumina samples which have been impregnated with different solution

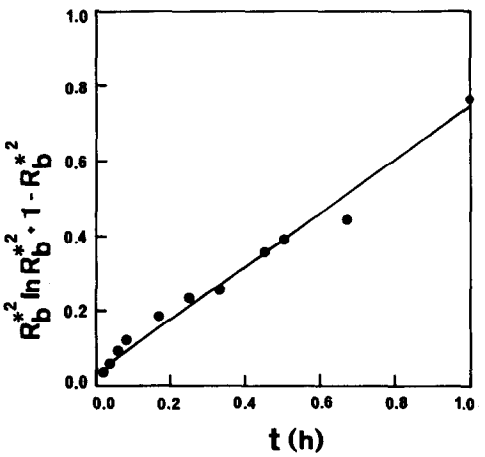

FIG. 3. Fitting of experimental data to Eq. (13).

TABLE 1

Experimental and Calculated Penetration Radii $R_b^* = R_b/R_0$ as a Function of Impregnation Time

Time (min)	Penetration radii	
	Experimental	Calculated
5	0.73 ± 0.03[a]	0.83
10	0.67 ± 0.04	0.74
15	0.63 ± 0.05	0.68
20	0.61 ± 0.03	0.62
30	0.51 ± 0.04	0.53
40	0.46 ± 0.07	0.45
60	0.26 ± 0.08	0.28
90	0.18 ± 0.16	0.0

Note. Impregnation bath concentration $C_0 = 0.5$ mol liter^{-1}.

[a] Mean values and standard deviations of 15 measurements.

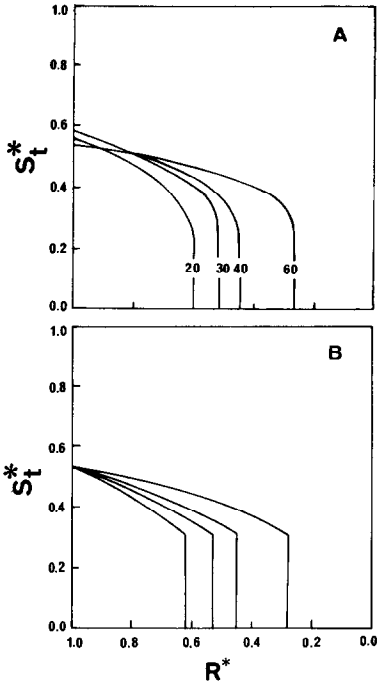

FIG. 4. Comparison between experimental (A) and calculated (B) copper concentration profiles for different impregnation times (20, 30, 40, and 60 min). Impregnation bath concentration 0.5 *M* $CuCl_2$.

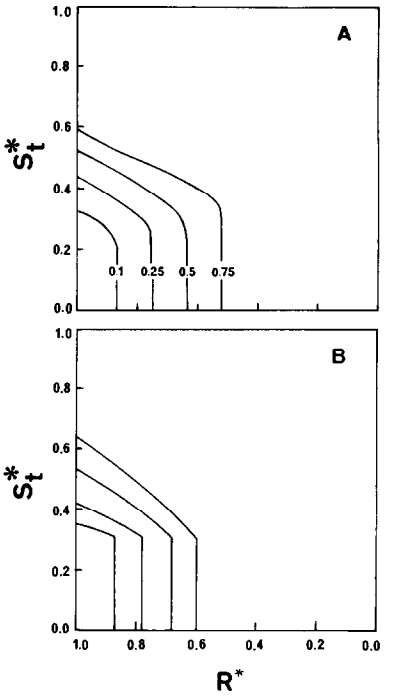

FIG. 5. Comparison between experimental (A) and calculated (B) copper concentration profiles for different impregnation bath concentration (0.1, 0.25, 0.5, and 0.75 *M* $CuCl_2$). Impregnation time 15 min.

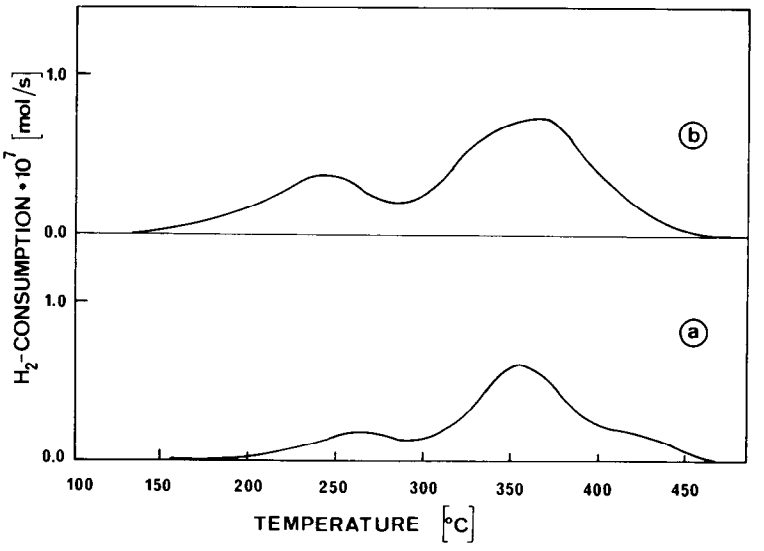

FIG. 6. TPR profiles measured for alumina pellets which have been impregnated for 15 min with different impregnation bath concentrations, C_0. (a) C_0 = 0.25 mol liter^{-1}; (b) C_0 = 0.5 mol liter^{-1}.

TABLE 2

Experimental and Calculated Total Metal Uptakes N_t as a Function of Impregnation Time

Time (min)	Total metal uptake (mol kg^{-1})	
	Experimental	Calculated
1	0.069 ± 0.004[a]	0.072
5	0.150 ± 0.012	0.140
10	0.198 ± 0.007	0.195
30	0.324 ± 0.015	0.318
60	0.445 ± 0.020	0.426
75	0.482[b]	0.469
90	0.528 ± 0.033	0.530

Note. Impregnation bath concentration C_0 = 0.5 mol liter^{-1}.

[a] Mean values and standard deviations of 12 measurements.

[b] Only one measurement.

concentrations (C_0 = 0.25 and 0.5 mol liter^{-1}). Both profiles indicate that two types of copper species of different reducibility are immobilized on the alumina. It is interesting to note that the fraction of the total hydrogen consumption due to copper species reduced at lower temperature is about twice as large for the alumina which has been impregnated with the impregnation solution of higher concentration (C_0 = 0.5 mol liter^{-1}).

DISCUSSION

The impregnation of γ-alumina with aqueous solutions of copper chloride is clearly shell-progressive in nature (*14*). The catalyst concentration profiles are readily modelled by accounting for two types of copper species—one formed by rapid irreversible immobilization and one formed by precipitation.

The model developed above is only applicable when the solution is rapidly evaporated from the pores, effectively "freezing" the location of the catalyst deposited by precipitation. The good agreement between measured and calculated copper concentration profiles indicates that the drying process did, in fact, not cause marked migration of the copper ions. This behaviour is, of course, not met under all possible drying conditions. The effect of drying rate on concentration profiles has been extensively discussed (*1*).

The assumption of a steady-state concentration profile and a constant flux between R_0 and R_b (Eq. (4)) greatly simplifies the diffusion–immobilization model. It is expected that this simplification can become critical, when the solute held in the pore fluid becomes appreciable compared to the amount adsorbed. For such conditions, it may become necessary to include an accumulation term in the model. Neglecting the accumulation term in the model would lead to the prediction of a too rapid uptake, in this case. At any rate, the generally good agreement between theory and experiment in our study indicates that a more complicated diffusion–immobilization model which includes an accumulation term, is not necessary to describe our impregnation experiments.

One noteworthy aspect of the model is that it predicts the existence of two types of copper species—one formed by irreversible adsorption and the other by precipitation during drying. This prediction is substantiated by the TPR measurements shown in Fig. 6, which exhibit two significant maxima for the hydrogen consumption rate, indicating the coexistence of two copper species with significantly different reducibilities.

Employing Eqs. (20)–(22) the fraction of the total copper uptake originating from precipitation (N_p^*/N_t^*) is calculated to be 0.15 for sample (a) and 0.29 for sample (b). This results together with the TPR profiles, indicate that the copper species reduced at lower temperature are most likely those originating from precipitation, since the fraction of the total hydrogen consumption due to the copper species reduced at lower temperature is also about two times larger for sample (b).

There is evidence that the two types of

copper in the unreduced form exhibit different activities and selectivities for oxychlorination (*22*). Less certain, but also possible, is that the two types of copper, following reduction, will exhibit different activities and selectivities for various metal-catalyzed reactions.

ACKNOWLEDGMENT

Thanks are due to Daniele Monti for carrying out the TPR measurements and critically reading the manuscript.

REFERENCES

1. Neimark, A. V., Kheifez, L. I., and Fenelonow, V. B., *Ind. Eng. Chem. Prod. Res. Dev.* **20,** 439 (1981).
2. Weisz, P. B., *Trans. Faraday Soc.* **63,** 1801 (1967).
3. Weisz, P. B., and Hicks, J. S., *Trans. Faraday Soc.* **63,** 1807 (1967).
4. Weisz, P. B., and Zollinger, H., *Trans. Faraday Soc.* **63,** 1815 (1967).
5. Harriott, P., *J. Catal.* **14,** 43 (1969).
6. Vincent, R. C., and Merill, R. P., *J. Catal.* **35,** 206 (1974).
7. Chen, H. C., and Anderson, R. B., *J. Catal.* **43,** 200 (1976).
8. Santacesaria, E., Galli, C., and Carra, S., *React. Kinet. Catal. Lett.* **6,** 301 (1977).
9. Melo, F., Cervello, J., and Hermana, E., *Chem. Eng. Sci.* **35,** 2165 (1980).
10. Melo, F., Cervello, J., and Hermana, E., *Chem. Eng. Sci.* **35,** 2175 (1980).
11. Komiyama, M., Merill, R. P., and Harnsberger, H. F., *J. Catal.* **63,** 35 (1980).
12. Machek, V., Hanika, J., Sporka, K., Ruzicka, V., Kunz, J., and Janacek, L., *in* "Preparation of Catalysts III" (B. Delmon, P. Grange, P. Jacobs, and G. Poncelet, Eds.), p. 69. Elsevier, Amsterdam, 1983.
13. Lee, S. Y., and Aris, R., *in* "Preparation of Catalysts III" (B. Delmon, P. Grange, P. Jacobs, and G. Poncelet, Eds.), p. 35. Elsevier, Amsterdam, 1983.
14. Ott, R. J., and Baiker, A., *in* "Preparation of Catalysts III" (B. Delmon, P. Grange, P. Jacobs, and G. Poncelet, Eds.), p. 685. Elsevier, Amsterdam, 1983.
15. Hill, A. V., *Proc. Roy. Soc. B* **104,** 39 (1928).
16. Crank, J., *Trans. Faraday Soc.* **53,** 1083 (1957).
17. Turkdogen, E. T., and Vinters, F. V., *Metall. Trans.* **2,** 3175 (1971).
18. Weisz, P. B., and Goodwin, R. D., *J. Catal.* **2,** 397 (1963).
19. Monti, D. M. A., and Baiker, A., *J. Catal.* **83,** 323 (1983).
20. Oeholm, L. W., *Fin. Kemistsamf. Medd.* **46,** 124 (1938).
21. Weisz, P. B., and Schwartz, A. B., *J. Catal.* **1,** 399 (1962).
22. Blanco, J., Fayos, J., Garcia de la Banda, J. F., and Soria, J., *J. Catal.* **31,** 257 (1973).